Robust Quantum Gates against Correlated Noise in Integrated Quantum Chips

Kangyuan Yi,[1,*] Yong-Ju Hai,[2,3,*] Kai Luo,[1,2] Ji Chu,[2,3] Libo Zhang,[2,3] Yuxuan Zhou,[1,2] Yao Song,[2,3] Song Liu,[2,3,4] Tongxing Yan,[2,3,4,†] Xiu-Hao Deng,[2,3,4,‡] Yuanzhen Chen,[1,2,4,§] and Dapeng Yu[1,2,3,4]

[1]*Department of Physics, Southern University of Science and Technology, Shenzhen 518055, China*

[2]*Shenzhen Institute for Quantum Science and Engineering, Southern University of Science and Technology, Shenzhen 518055, China*

[3]*International Quantum Academy (SIQA), Shenzhen 518048, China*

[4]*Guangdong Provincial Key Laboratory of Quantum Science and Engineering, Southern University of Science and Technology, Shenzhen, 518055, China*

(Received 3 January 2024; accepted 22 May 2024; published 20 June 2024)

As quantum circuits become more integrated and complex, additional error sources that were previously insignificant start to emerge. Consequently, the fidelity of quantum gates benchmarked under pristine conditions falls short of predicting their performance in realistic circuits. To overcome this problem, we must improve their robustness against pertinent error models besides isolated fidelity. Here, we report the experimental realization of robust quantum gates in superconducting quantum circuits based on a geometric framework for diagnosing and correcting various gate errors. Using quantum process tomography and randomized benchmarking, we demonstrate robust single-qubit gates against quasistatic noise and spatially correlated noise in a broad range of strengths, which are common sources of coherent errors in large-scale quantum circuits. We also apply our method to nonstatic noises and to realize robust two-qubit gates. Our Letter provides a versatile toolbox for achieving noise-resilient complex quantum circuits.

DOI: 10.1103/PhysRevLett.132.250604

Quantum logic gates are typically benchmarked in isolation under pristine conditions to obtain high fidelities surpassing fault-tolerance thresholds of quantum error correction (QEC) codes [1–3]. However, when deployed in large-scale quantum circuits, additional noise channels emerge, leading to errors that are absent or negligible in the isolated gate setting [4–7]. These noises arise from effects like crosstalk, control imperfection, and correlated noise [8–14], leading to complex errors that are difficult to benchmark in isolation. Consequently, the gate fidelity measured under well-controlled conditions fails to faithfully predict performance in real circuits. To overcome this challenge, we need to rigorously evaluate the gate robustness against pertinent error models beyond isolated fidelity [15].

Robust gates exhibit built-in noise resilience through careful pulse shaping, making them well-suited for constructing complex quantum algorithms [16–18]. In particular, they help correct coherent errors of significant spatiotemporal correlations, which are known to pose great challenges for QEC [19–21]. Recently, a geometric technique has been developed to design smooth and short-duration robust control pulses (RCPs) that suppress errors from general noise processes in multiple directions [22–26]. The RCPs are constructed by mapping the noisy quantum evolution onto error curves in a parameter space. The topology of these curves, such as their closeness, directly determines the gate robustness, while the local geometric properties like curvature and torsion are linked to parameters of the control Hamiltonian. This framework provides both an intuitive picture of noisy quantum evolution and a systematic tool for RCP optimization.

In this Letter, we experimentally demonstrate robust quantum gates based on the above RCPs using superconducting quantum circuits. After a concise introduction to the design principles, we report experimental results on quantum gates that are much more fault-tolerant against coherent errors resulting from generic noises with components in multiple directions than conventional dynamical gates. More importantly, we find that our gates significantly suppress the pernicious buildup of coherent errors in long circuits subjected to temporally correlated noise, leading to substantially enhanced overall circuit performance and worst-case fidelity, which may benefit fault-tolerant QEC.

We start with the Hamiltonian of a qubit driven by a control field $H_c(t)$ and subjected to a generic noise $V(t)$: $H(t) = H_0 + H_c(t) + V(t)$, where H_0 is the free-qubit Hamiltonian. The noiseless evolution is $U_0(t) = \mathcal{T}\exp\{-i\int_0^t(H_0 + H_c(\tau))d\tau\}$ ($\mathcal{T}$ stands for time ordering). We define an error unitary as $U_e(t) = \mathcal{T}\exp\{-i\int_0^t d\tau H_I(\tau)\}$, where $H_I = U_0^\dagger V U_0$ is the noise in the interaction frame determined by U_0. Since the total evolution unitary can be decomposed as $U = U_0 U_e$ [see Supplemental Material (SM) [27]], it then follows that to realize robust quantum gates, one simply engineers $H_c(t)$ to obtain a target gate with

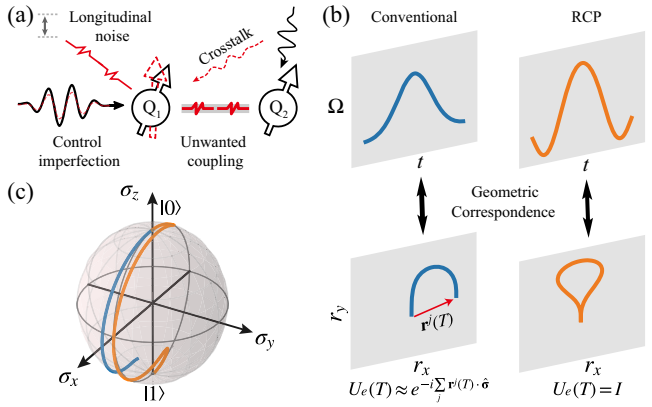

FIG. 1. (a) Schematics of the realistic noisy environment of qubits. (b) Upper panel: schematics of the control signal envelopes, $\Omega(t)$, for a Gaussian pulse (blue) and an RCP (orange). Lower panel: error curves of the two pulses derived in our geometric framework, in the presence of a generic noise as given in the main text. The red vector $\mathbf{r}^j(T)$ indicates a finite susceptibility to noise, corresponding to a compromised robustness. Conversely, a closed error curve in the RCP case (orange) yields a robust gate to the first order. (c) Dynamics of an X^π gate for an initial state of $|0\rangle$ using Gaussian pulse (blue) and RCP (orange) in the presence of a static frequency detuning noise.

a duration of T, $U_0(T) = U_{\text{target}}$, while eliminating the impact of noise at the end of evolution, i.e., $U_e(T) = I$.

To proceed, we write the noise term as $V(t) = \sum_{j,k} \epsilon_k^j v_k^j(t)\sigma_k$, where $k = x, y, z$ and ϵ_k^j is a time-independent amplitude of the k component for the jth noise source and v_k^j is its possibly time-dependent profile. σ_k are the Pauli matrices. Hereafter, we reserve the upper index j for numbering different noise sources. Some of the possible origins of the noises are illustrated in Fig. 1(a). The error unitary $U_e(t)$ can be calculated using a perturbative expansion (see SM [27]). Up to the leading order, one has $U_e(t) \approx e^{-i\sum_j \Phi^j(t)}$, where $\Phi^j(t)$ is a matrix associated with the jth noise source and can be expressed as $\Phi^j(t) = \mathbf{r}^j(t)\cdot\hat{\boldsymbol{\sigma}}$. Here, $\mathbf{r}^j(t)$ is a vector that traces out a three-dimensional curve as t evolves. This curve describes the accumulated error of the jth noise on the evolution unitary and is thus named as an "error curve." The geometric correspondence between the noisy quantum dynamics and the error curves enables a straightforward and intuitive approach to designing robust quantum control. For example, the "error distance" $R^j(t) = \|\mathbf{r}^j(t)\|$ measures the susceptibility of the quantum dynamics to the jth noise source and is thus a natural metric for characterizing the robustness of the corresponding quantum operation. Essentially, a robust control requires the error distances to vanish at the end of gate operation, i.e., $R^j(T) = 0$. With this condition met, one has $\Phi^j(T) = 0$ and thus $U_e(T) = I$. We illustrate this robust control framework in Figs. 1(b) and 1(c). Further details of the construction of robust control pulses can be found in the SM [27] and Ref. [26].

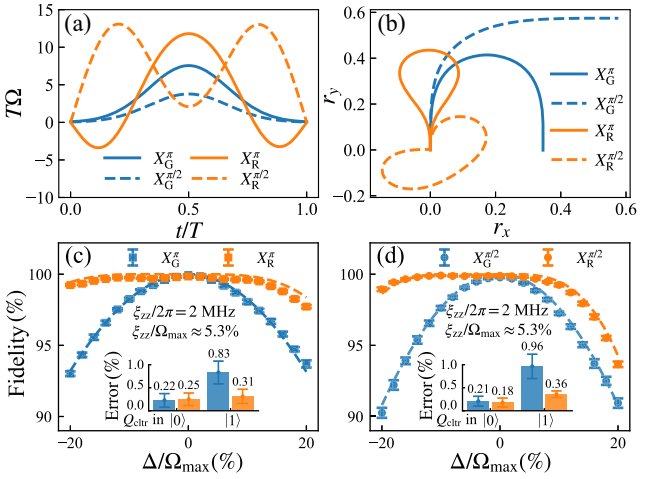

FIG. 2. Robustness of representative single-qubit gates exposed to a static noise in the z direction. (a) Pulse envelopes of two Gaussian (G) gates X_G^π, $X_G^{\pi/2}$ and two robust (R) gates X_R^π, $X_R^{\pi/2}$. For comparison, the horizontal axis is set to normalized time, with the actual gate time being $T = 32$, 16, 50, 55 ns, respectively. The vertical axis represents a dimensionless quantity of $T\Omega(t)$ where $\Omega(t)$ is the actual time-dependent envelope. The maximal amplitude of the pulses is $\Omega_{\max}/2\pi = 37.5$ MHz for all four gates. (b) The error curves of the four pulses in (a) for the frequency noise ($\mathbf{r}^\Delta$). (c),(d) Main panel: gate fidelity characterized by QPT for the four gates. The experimental data (symbols) fit the numerical simulations (dashed lines) well. Error bars are the standard deviation. Note that all the gates here are implemented with DRAG [70,71] to suppress the leakage. More details about the simulation and experiment are given in the SM [27]. Insets: gate error determined by QPT for an X^π and an $X^{\pi/2}$ gates using the RCP and Gaussian pulses in the presence of a ZZ interaction.

We have performed experiments on different superconducting quantum processors and obtained similar results. The data presented here were all acquired on a processor that consists of eight transmon [65,66] qubits arranged in a circle. Each qubit has a fixed frequency and is connected to the two nearest qubits via couplers that are also transmons but with tunable frequencies. More detailed information about this processor can be found in SM [27].

We first demonstrate robust single-qubit quantum gates against quasistatic noise in the z direction. For a transmon qubit, an equivalent quasistatic noise can be readily generated by purposely driving the qubit at a detuned frequency, leading to an effective Hamiltonian $H = 1/2\Omega(t)\sigma_x + 1/2\Delta\sigma_z$, where $\Omega(t)$ and Δ are pulse amplitude and frequency detuning, respectively. Figure 2 shows a representative dataset where the performance of four different quantum gates are compared using the standard quantum process tomography (QPT) [67–69], two using conventional Gaussian drives, and the other two using RCPs.

We also benchmark gate performance in the presence of a ZZ-type of crosstalk between neighboring qubits, which is a typical source for spatially correlated errors in

multiqubit circuits. For this purpose, two qubits and a tunable coupler are used. The coupler is tuned to induce a variable ZZ interaction between the two qubits. Consequently, the target qubit to be benchmarked feels a disturbance that depends on the state of the control qubit. The insets of Figs. 2(c) and 2(d) plot the errors of an X^{π} and an $X^{\pi/2}$ gates using the RCP and Gaussian pulses for a ZZ interaction of 2 MHz, which corresponds to a relative noise magnitude of 5.3% ($\xi_{ZZ}/\Omega_{\max}$). As the control qubit is set to different states, the gate performance of the target qubit is much more robust in the case of RCP pulses. A similar robust profile against the ZZ interaction using X_R^{π} gate was also observed in the fixed-frequency transmon system with always-on couplings [72].

Following the same principles, one can readily design robust quantum gates for more realistic scenarios where noise and error appear in all three directions. Let us consider the following Hamiltonian $H = \frac{1}{2}(1+\epsilon)\Omega_x(t)\sigma_x + \frac{1}{2}(1+\epsilon)\Omega_y(t)\sigma_y + \frac{1}{2}\Delta\sigma_z$, where both a control amplitude noise ϵ and a frequency detuning Δ are present simultaneously. Using the aforementioned protocol, we construct the RCP for an X^{π} gate, as shown in Fig. 3(a). Notice that the pulse now has both x and y components, which is necessary to suppress noises in all three directions. Experimental and simulated results of the gate fidelity extracted by QPT are plotted in Fig. 3(c). In the SM [27], we further discuss robust gates that can battle against errors due to noises with independent components in three directions, as well as the error induced by residual ZZ coupling among qubits, which is notoriously harmful and difficult to handle in solid-state quantum systems.

The results shown in Figs. 2 and 3 clearly demonstrate the superior noise resilience of our robust gates. Besides this advantage, we also note that our RCPs are smooth pulses with relatively short durations compared to most other schemes of robust quantum gates. These features bring two important benefits. First, smooth pulses are more friendly for experimental implementation and also more likely to deliver reproducible performance. On the contrary, many existing protocols of robust gates adopt piecewise signals, often accompanied by abrupt jumps in parameters between different segments. Second, short duration always means less error due to decoherence. To further illustrate the practicality of RCPs, Fig. 3(d) numerically compares the performance of an RCP and a Gaussian X^{π} gate in the presence of decoherence. It is clear that in a significant portion of the parameter space, RCPs outperform the Gaussian pulse by a large margin. This simulation is supported by the experimental results (see SM [27] for a detailed comparison).

As discussed in the introduction, fidelity benchmarked by QPT alone does not faithfully herald the gate and circuit performance in realistic quantum circuits. For example, it is well-known that noises of long correlations produce errors that accumulate coherently as a circuit progresses. The

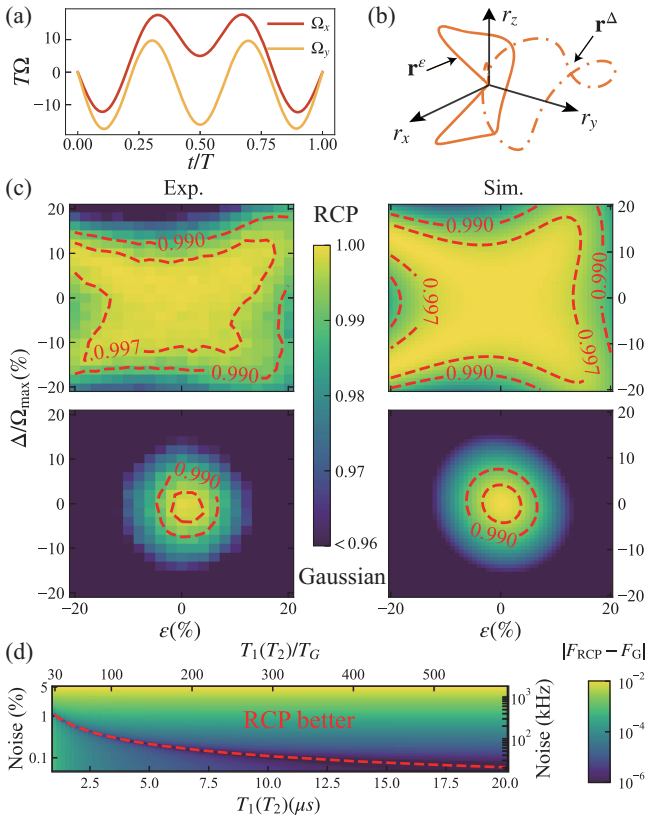

FIG. 3. Robust gate against both control imperfection ϵ and frequency detuning Δ. (a) x and y components of the RCP for a robust X^{π} gate with a duration of $T_R = 80$ ns. (b) Illustration of the two error curves ($\mathbf{r}^{\epsilon}$ and $\mathbf{r}^{\Delta}$) of the RCP in (a) for the amplitude and frequency noises. (c) QPT fidelities for the RCP (upper) and Gaussian (lower) pulse as a function of noise amplitudes ϵ and Δ. Results from numerical simulation (right) and experimental data (left) are in good agreement. (d) The numerical result of the absolute difference of gate fidelity $|F_{\mathrm{RCP}} - F_G|$ for the X^{π} gate versus noise amplitude and decoherence times, where the RCP outperforms the Gaussian pulse in a broad region (above the red dashed line). Here the assumption is that $\epsilon = \Delta/\Omega_{\max}$ (noise) and $T_1 = T_2$. The durations of the two gates (T_R, T_G) are 80 and 34 ns, respectively.

detrimental effect of such coherent errors becomes increasingly more prominent as the circuit depth grows. More severely, such coherent errors are difficult to perceive and correct. They thus pose great challenges for both QEC and noisy intermediate-scale quantum applications [19–21]. Common sources of such coherent errors widely observed in different platforms include non-Markovian noise of significant low-frequency components, long-term drift in systems, control imperfection, miscalibration, crosstalk, and unwanted qubit-qubit coupling of large characteristic times. In the following, we demonstrate how robust quantum gates, combined with other techniques, can help correct such temporally correlated coherent errors. For this purpose, we perform experiments on Clifford-based randomized benchmarking (RB) [73–75] in the presence of a

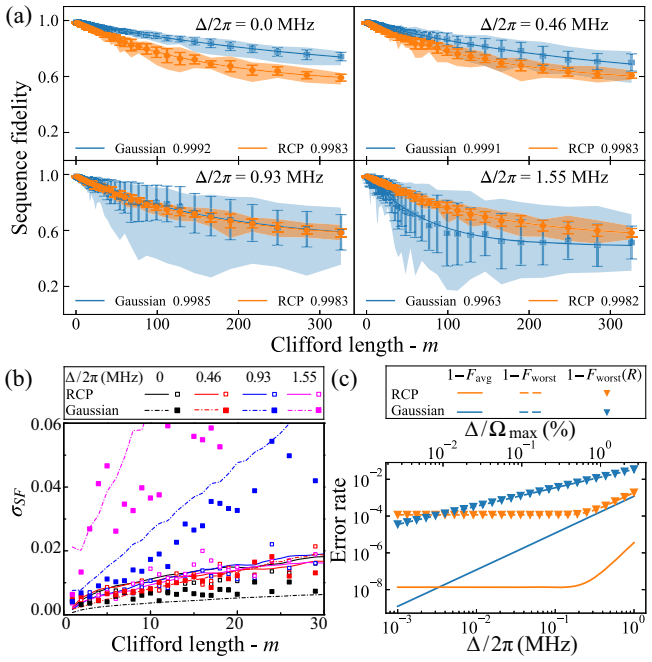

FIG. 4. (a) Reference RB measurements are performed at different values of Δ. Each measurement consists of 20 sequences of randomly chosen Clifford gates. Lines are fittings to the sequence fidelity by a formula $F = Ap^m + B$. The average fidelity per gate (lower legend in each panel) is given by $F_{\text{avg}} = 1 - (1-p)/3.75$ [75]. Error bars are the standard deviation and the shaded areas indicate the range of data. (b) Variance of sequence fidelity as a function of Clifford length. Lines are numerical simulations (see SM [27]), and symbols are experimental results extracted from data in (a). (c) Numerical result of average and worst-case errors of the X^{π} gate. Lines and symbols for the worst-case errors are calculated using the diamond norm solver and robustness measure respectively (see SM [27]).

static frequency detuning, which represents an extreme case of temporal correlation. The qubit frequency is first calibrated as ω_{q0} with its neighboring couplers tuned far away. Then the frequency of one coupler is brought close to ω_{q0}, so the actual frequency of the qubit becomes $\omega_q = \omega_{q0} - \Delta$. We determine Δ as a function of the bias applied to the coupler, then perform reference RB measurements at different values of Δ. All gates in the RB sequences are designed assuming the frequency of the qubit being fixed at ω_{q0}. Therefore, Δ appears as a static detuning.

Figure 4(a) shows RB results obtained at different values of Δ. At $\Delta = 0$, the Gaussian case outperforms slightly due to a shorter average gate time, thus, less error resulting from decoherence. Also, the small oscillation of RCP's variance indicates some remaining correlated noises that probably come from the miscalibration of slightly more complex pulse shapes. As Δ increases, the performance of the robust gate sequences remains nearly unchanged, whereas the Gaussian sequences start to exhibit much-widened variances. Even though nominal high values of average fidelity per gate can still be extracted, they are definitely insufficient for evaluating the overall circuit performance. For example, the average error per gate for the Gaussian sequence is ∼0.08% for $\Delta/2\pi = 0$ MHz, mainly caused by decoherence. It increases to ∼0.15% for $\Delta/2\pi = 0.93$ MHz. However, the impact of such a seemingly small extra error resulting from the static detuning on the circuit performance is much more detrimental than errors due to decoherence. We also note that the maximum $\Delta/2\pi$ value studied here (1.55 MHz) corresponds to a relative frequency detuning of 0.023% ($\Delta_{\max}/\omega_{q0}$) and a relative noise magnitude of 4.1% ($\Delta_{\max}/\Omega_{\max}$), both being reasonably small in reality. But their impact cannot be neglected at all.

The built-in randomization in RB sequences is known to convert coherent errors induced by noises of long correlations into incoherent ones. Qualitatively speaking, this process is similar to a random walk in real space, where the distance of the walker drifting away from the starting point is determined by both the randomness in its moving pattern and the step size. In the current case, the step size corresponds to the average error accumulated in an individual gate, and the sequence fidelity variance resembles the distribution of a random walker's distance from its starting point. In Fig. 4(b), we plot the variance of sequence fidelity σ_{SF} as a function of the Clifford length m. For the RB sequences using RCPs, the σ_{SF}-m relation is nearly independent of the detuning Δ, indicating that the dominant error accumulated in individual gates comes from decoherence, in sharp contrast to the Gaussian case. Of course, unlike a random walk in an Euclidean space, the accumulation of coherent errors in a quantum circuit proceeds in its Hilbert space and is described by the corresponding Pauli transfer matrices. The unique mathematical framework in the quantum case makes it difficult to carry out a quantitative analysis. More discussion on this issue is given in the SM [27].

Above, we show that combining randomization and robust quantum gates helps correct coherent errors induced by static detuning. It is reasonable to expect that coherent errors due to other physical processes with a quasistatic nature can also be corrected this way. On the other hand, coherent errors resulting from a generic noise with nontrivial time dependence but small correlation length, such as the control imperfection studied in Fig. 3, can be already handled by robust quantum gates without the need for randomization. Moving onto realistic quantum circuits where coherent errors of different correlation lengths exist and an intrinsic randomization as in RB is not available, one can then combine robust quantum gates with other techniques for mitigating coherent errors developed from a circuit perspective. One simple example is the so-called randomized compiling [76–79], in which effective randomization converts coherent errors into incoherent ones and can be routinely introduced into quantum circuits without sufficient built-in randomness.

The large variance observed in the RB sequences of Gaussian pulses has another severe implication: it means that the worst-case error of Gaussian gates is significantly larger in the presence of coherent errors [21,80,81]. Within our theoretical framework, the worst-case error can be easily calculated from the robustness measure, that is, the error distance (see SM [27]). Figure 4(c) plots the simulated average and worst-case errors of an X^{π} gate for both Gaussian and RCP pulses. As the robustness of the worst-case error is concerned, the advantage of RCPs over the Gaussian pulses is even more prominent than only considering the average error. Since the worst-case error determines the fault tolerance of QEC codes [21,82,83], our results are particularly beneficial for QEC applications.

Finally, we note that our protocol not only can help correct coherent errors as shown above, but it can also be used to realize robust control beyond single qubits more directly. In SM [27], we show that an iSWAP gate constructed using RCPs also exhibits excellent robustness against frequency fluctuations. Generalization for different two-qubit gate schemes in a variety of platforms is also straightforward.

To conclude, we have demonstrated the effectiveness of robust single-qubit gates in correcting errors caused by spatially correlated noises, including unwanted ZZ interaction, crosstalk, and temporally correlated noises, including frequency variation, pulse deformation in various directions and with diverse strengths. These noises are related to realistic physical processes observed in different platforms and cause coherent errors that are difficult to identify and correct. We have presented a good fit of experimental and theoretical results of process tomography. Our RB measurements have shown the suppression of the coherence of errors and reduction of the worst-case error. Our results offer a promising approach to combat the increasing challenges associated with correlated noises in integrated quantum chips. Additionally, when combined with other error mitigation methods, the techniques reported here help reduce such errors and may benefit both QEC and noisy intermediate-scale quantum applications. Therefore, we propose an alternative path toward achieving high-quality large-scale quantum computing.

This work was supported by the Key-Area Research and Development Program of Guangdong Province (No. 2018B030326001), the National Natural Science Foundation of China (No. 12074166 and No. 12004162), the Guangdong Provincial Key Laboratory (No. 2019B121203002), and the Shenzhen Science and Technology Program (KQTD20200820113010023).

*These authors contributed equally to this work.
†Corresponding author: yantx@sustech.edu.cn
‡Corresponding author: dengxh@sustech.edu.cn
§Corresponding author: chenyz@sustech.edu.cn

[1] B. Cheng *et al.*, Front. Phys. **18**, 21308 (2023).
[2] K. Bharti *et al.*, Rev. Mod. Phys. **94**, 015004 (2022).
[3] Y. Alexeev *et al.*, PRX Quantum **2**, 017001 (2021).
[4] C. Monroe, W. C. Campbell, L.-M. Duan, Z.-X. Gong, A. V. Gorshkov, P. W. Hess, R. Islam, K. Kim, N. M. Linke, G. Pagano, P. Richerme, C. Senko, and N. Y. Yao, Rev. Mod. Phys. **93**, 025001 (2021).
[5] D. Bluvstein, H. Levine, G. Semeghini, T. T. Wang, S. Ebadi, M. Kalinowski, A. Keesling, N. Maskara, H. Pichler, M. Greiner, V. Vuletić, and M. D. Lukin, Nature (London) **604**, 451 (2022).
[6] F. Arute *et al.*, Nature (London) **574**, 505 (2019).
[7] S. Bravyi, S. Sheldon, A. Kandala, D. C. Mckay, and J. M. Gambetta, Phys. Rev. A **103**, 042605 (2021).
[8] P. Mundada, G. Zhang, T. Hazard, and A. Houck, Phys. Rev. Appl. **12**, 054023 (2019).
[9] S. Sheldon, E. Magesan, J. M. Chow, and J. M. Gambetta, Phys. Rev. A **93**, 060302(R) (2016).
[10] J. M. Gambetta, A. D. Córcoles, S. T. Merkel, B. R. Johnson, J. A. Smolin, J. M. Chow, C. A. Ryan, C. Rigetti, S. Poletto, T. A. Ohki, M. B. Ketchen, and M. Steffen, Phys. Rev. Lett. **109**, 240504 (2012).
[11] M. D. Reed, L. DiCarlo, S. E. Nigg, L. Sun, L. Frunzio, S. M. Girvin, and R. J. Schoelkopf, Nature (London) **482**, 382 (2012).
[12] R. C. Bialczak, R. McDermott, M. Ansmann, M. Hofheinz, N. Katz, E. Lucero, M. Neeley, A. D. O'Connell, H. Wang, A. N. Cleland, and J. M. Martinis, Phys. Rev. Lett. **99**, 187006 (2007).
[13] S. Gustavsson, J. Bylander, F. Yan, W. D. Oliver, F. Yoshihara, and Y. Nakamura, Phys. Rev. B **84**, 014525 (2011).
[14] D. A. Rower *et al.*, Phys. Rev. Lett. **130**, 220602 (2023).
[15] A. W. Harrow and M. A. Nielsen, Phys. Rev. A **68**, 012308 (2003).
[16] G. Dridi, K. Liu, and S. Guérin, Phys. Rev. Lett. **125**, 250403 (2020).
[17] B.-J. Liu, Y.-S. Wang, and M.-H. Yung, Phys. Rev. Res. **3**, L032066 (2021).
[18] N. H. Le, M. Cykiert, and E. Ginossar, npj Quantum Inf. **9**, 1 (2023).
[19] R. Harper and S. T. Flammia, PRX Quantum **4**, 040311 (2023).
[20] J. K. Iverson and J. Preskill, New J. Phys. **22**, 073066 (2020).
[21] R. Kueng, D. M. Long, A. C. Doherty, and S. T. Flammia, Phys. Rev. Lett. **117**, 170502 (2016).
[22] J. Zeng, C. H. Yang, A. S. Dzurak, and E. Barnes, Phys. Rev. A **99**, 052321 (2019).
[23] W. Dong, F. Zhuang, S. E. Economou, and E. Barnes, PRX Quantum **2**, 030333 (2021).
[24] D. Buterakos, S. Das Sarma, and E. Barnes, PRX Quantum **2**, 010341 (2021).
[25] X.-H. Deng, Y.-J. Hai, J.-N. Li, and Y. Song, arXiv: 2103.08169.
[26] Y.-J. Hai, J. Li, J. Zeng, D. Yu, and X.-H. Deng, arXiv: 2210.14521.
[27] See Supplemental Material at http://link.aps.org/supplemental/10.1103/PhysRevLett.132.250604, which includes Refs. [28–64], for additional information about the

experimental setup, samples, and detailed discussions of the numerical simulations and data analysis.
[28] S. Blanes, F. Casas, J. Oteo, and J. Ros, Phys. Rep. **470**, 151 (2009).
[29] L. H. Pedersen, N. M. Møller, and K. Mølmer, Phys. Lett. A **367**, 47 (2007).
[30] S. Krinner, S. Lazar, A. Remm, C. K. Andersen, N. Lacroix, G. J. Norris, C. Hellings, M. Gabureac, C. Eichler, and A. Wallraff, Phys. Rev. Appl. **14**, 024042 (2020).
[31] T.-Q. Cai, X.-Y. Han, Y.-K. Wu, Y.-L. Ma, J.-H. Wang, Z.-L. Wang, H.-Y. Zhang, H.-Y. Wang, Y.-P. Song, and L.-M. Duan, Phys. Rev. Lett. **127**, 060505 (2021).
[32] X. Xue, M. Russ, N. Samkharadze, B. Undseth, A. Sammak, G. Scappucci, and L. M. K. Vandersypen, Nature (London) **601**, 343 (2022).
[33] Y. Sung, L. Ding, J. Braumüller, A. Vepsäläinen, B. Kannan, M. Kjaergaard, A. Greene, G. O. Samach, C. McNally, D. Kim *et al.*, Phys. Rev. X **11**, 021058 (2021).
[34] Y. R. Sanders, J. J. Wallman, and B. C. Sanders, New J. Phys. **18**, 012002 (2015).
[35] J. Johansson, P. Nation, and F. Nori, Comput. Phys. Commun. **184**, 1234 (2013).
[36] J. Chu *et al.*, Nat. Phys. **19**, 126 (2023).
[37] K. Luo, W. Huang, Z. Tao, L. Zhang, Y. Zhou, J. Chu, W. Liu, B. Wang, J. Cui, S. Liu, F. Yan, M.-H. Yung, Y. Chen, T. Yan, and D. Yu, Phys. Rev. Lett. **130**, 030603 (2023).
[38] J. Zhang, R. Laflamme, and D. Suter, Phys. Rev. Lett. **109**, 100503 (2012).
[39] G. Feng, G. Xu, and G. Long, Phys. Rev. Lett. **110**, 190501 (2013).
[40] Y. Xu, W. Cai, Y. Ma, X. Mu, L. Hu, T. Chen, H. Wang, Y. P. Song, Z.-Y. Xue, Z. Q. Yin, and L. Sun, Phys. Rev. Lett. **121**, 110501 (2018).
[41] P. J. J. O'Malley *et al.*, Phys. Rev. Appl. **3**, 044009 (2015).
[42] L. Ding, M. Hays, Y. Sung, B. Kannan, J. An, A. Di Paolo, A. H. Karamlou, T. M. Hazard, K. Azar, D. K. Kim, B. M. Niedzielski, A. Melville, M. E. Schwartz, J. L. Yoder, T. P. Orlando, S. Gustavsson, J. A. Grover, K. Serniak, and W. D. Oliver, Phys. Rev. X **13**, 031035 (2023).
[43] J. J. Burnett, A. Bengtsson, M. Scigliuzzo, D. Niepce, M. Kudra, P. Delsing, and J. Bylander, npj Quantum Inf. **5**, 1 (2019).
[44] A. Vepsäläinen, R. Winik, A. H. Karamlou, J. Braumüller, A. D. Paolo, Y. Sung, B. Kannan, M. Kjaergaard, D. K. Kim, A. J. Melville, B. M. Niedzielski, J. L. Yoder, S. Gustavsson, and W. D. Oliver, Nat. Commun. **13**, 1932 (2022).
[45] P. V. Klimov *et al.*, Phys. Rev. Lett. **121**, 090502 (2018).
[46] S. Schlör, J. Lisenfeld, C. Müller, A. Bilmes, A. Schneider, D. P. Pappas, A. V. Ustinov, and M. Weides, Phys. Rev. Lett. **123**, 190502 (2019).
[47] J. Lisenfeld, G. J. Grabovskij, C. Müller, J. H. Cole, G. Weiss, and A. V. Ustinov, Nat. Commun. **6**, 6182 (2015).
[48] J. Lisenfeld, A. Bilmes, A. Megrant, R. Barends, J. Kelly, P. Klimov, G. Weiss, J. M. Martinis, and A. V. Ustinov, npj Quantum Inf. **5**, 1 (2019).
[49] K. X. Wei, E. Magesan, I. Lauer, S. Srinivasan, D. F. Bogorin, S. Carnevale, G. A. Keefe, Y. Kim, D. Klaus, W. Landers, N. Sundaresan, C. Wang, E. J. Zhang, M. Steffen, O. E. Dial, D. C. McKay, and A. Kandala, Phys. Rev. Lett. **129**, 060501 (2022).
[50] S. Krinner, P. Kurpiers, B. Royer, P. Magnard, I. Tsitsilin, J.-C. Besse, A. Remm, A. Blais, and A. Wallraff, Phys. Rev. Appl. **14**, 044039 (2020).
[51] R. S. Gupta, N. Sundaresan, T. Alexander, C. J. Wood, S. T. Merkel, M. B. Healy, M. Hillenbrand, T. Jochym-O'Connor, J. R. Wootton, T. J. Yoder, A. W. Cross, M. Takita, and B. J. Brown, Nature (London) **625**, 259 (2024).
[52] E. J. Zhang *et al.*, Sci. Adv. **8**, eabi6690 (2022).
[53] Z. Chen *et al.* (Google Quantum AI Collaboration), Nature (London) **595**, 383 (2021).
[54] D. Szombati, A. Gomez Frieiro, C. Müller, T. Jones, M. Jerger, and A. Fedorov, Phys. Rev. Lett. **124**, 070401 (2020).
[55] T. F. Watson, S. G. J. Philips, E. Kawakami, D. R. Ward, P. Scarlino, M. Veldhorst, D. E. Savage, M. G. Lagally, M. Friesen, S. N. Coppersmith, M. A. Eriksson, and L. M. K. Vandersypen, Nature (London) **555**, 633 (2018).
[56] E. J. Connors, J. Nelson, L. F. Edge, and J. M. Nichol, Nat. Commun. **13**, 940 (2022).
[57] M. T. Madzik, T. D. Ladd, F. E. Hudson, K. M. Itoh, A. M. Jakob, B. C. Johnson, J. C. McCallum, D. N. Jamieson, A. S. Dzurak, A. Laucht, and A. Morello, Sci. Adv. **6**, eaba3442 (2020).
[58] H. Levine, A. Keesling, A. Omran, H. Bernien, S. Schwartz, A. S. Zibrov, M. Endres, M. Greiner, V. Vuletić, and M. D. Lukin, Phys. Rev. Lett. **121**, 123603 (2018).
[59] S. de Léséleuc, D. Barredo, V. Lienhard, A. Browaeys, and T. Lahaye, Phys. Rev. A **97**, 053803 (2018).
[60] M. Saffman, J. Phys. B **49**, 202001 (2016).
[61] S. Jandura, J. D. Thompson, and G. Pupillo, PRX Quantum **4**, 020336 (2023).
[62] C. Done, G. Madejski, R. Mushotzky, T. Turner, K. Koyama, and H. Kunieda, Astrophys. J. **400**, 138 (1992).
[63] J. Timmer and M. König, Astron. Astrophys. **300**, 707 (1995), https://articles.adsabs.harvard.edu//full/1995A%26A...300..707T/0000707.000.html.
[64] J. Bylander, S. Gustavsson, F. Yan, F. Yoshihara, K. Harrabi, G. Fitch, D. G. Cory, Y. Nakamura, J.-S. Tsai, and W. D. Oliver, Nat. Phys. **7**, 565 (2011).
[65] J. Koch, T. M. Yu, J. Gambetta, A. A. Houck, D. I. Schuster, J. Majer, A. Blais, M. H. Devoret, S. M. Girvin, and R. J. Schoelkopf, Phys. Rev. A **76**, 042319 (2007).
[66] J. A. Schreier, A. A. Houck, J. Koch, D. I. Schuster, B. R. Johnson, J. M. Chow, J. M. Gambetta, J. Majer, L. Frunzio, M. H. Devoret, S. M. Girvin, and R. J. Schoelkopf, Phys. Rev. B **77**, 180502(R) (2008).
[67] M. A. Nielsen and I. L. Chuang, *Quantum Computation and Quantum Information: 10th Anniversary Edition* (Cambridge University Press, Cambridge, England, 2010).
[68] J. L. O'Brien, G. J. Pryde, A. Gilchrist, D. F. V. James, N. K. Langford, T. C. Ralph, and A. G. White, Phys. Rev. Lett. **93**, 080502 (2004).
[69] J. M. Chow, J. M. Gambetta, L. Tornberg, J. Koch, L. S. Bishop, A. A. Houck, B. R. Johnson, L. Frunzio, S. M. Girvin, and R. J. Schoelkopf, Phys. Rev. Lett. **102**, 090502 (2009).

[70] F. Motzoi, J. M. Gambetta, P. Rebentrost, and F. K. Wilhelm, Phys. Rev. Lett. **103**, 110501 (2009).
[71] J. M. Gambetta, F. Motzoi, S. T. Merkel, and F. K. Wilhelm, Phys. Rev. A **83**, 012308 (2011).
[72] S. Watanabe, Y. Tabuchi, K. Heya, S. Tamate, and Y. Nakamura, Phys. Rev. A **109**, 012616 (2024).
[73] E. Knill, D. Leibfried, R. Reichle, J. Britton, R. B. Blakestad, J. D. Jost, C. Langer, R. Ozeri, S. Seidelin, and D. J. Wineland, Phys. Rev. A **77**, 012307 (2008).
[74] E. Magesan, J. M. Gambetta, B. R. Johnson, C. A. Ryan, J. M. Chow, S. T. Merkel, M. P. da Silva, G. A. Keefe, M. B. Rothwell, T. A. Ohki, M. B. Ketchen, and M. Steffen, Phys. Rev. Lett. **109**, 080505 (2012).
[75] E. Magesan, J. M. Gambetta, and J. Emerson, Phys. Rev. A **85**, 042311 (2012).
[76] J. J. Wallman and J. Emerson, Phys. Rev. A **94**, 052325 (2016).
[77] M. Urbanek, B. Nachman, V. R. Pascuzzi, A. He, C. W. Bauer, and W. A. de Jong, Phys. Rev. Lett. **127**, 270502 (2021).
[78] A. Hashim, R. K. Naik, A. Morvan, J.-L. Ville, B. Mitchell, J. M. Kreikebaum, M. Davis, E. Smith, C. Iancu, K. P. O'Brien, I. Hincks, J. J. Wallman, J. Emerson, and I. Siddiqi, Phys. Rev. X **11**, 041039 (2021).
[79] Y. Gu, Y. Ma, N. Forcellini, and D. E. Liu, Phys. Rev. Lett. **130**, 250601 (2023).
[80] H. Ball, T. M. Stace, S. T. Flammia, and M. J. Biercuk, Phys. Rev. A **93**, 022303 (2016).
[81] C. L. Edmunds, C. Hempel, R. J. Harris, V. Frey, T. M. Stace, and M. J. Biercuk, Phys. Rev. Res. **2**, 013156 (2020).
[82] P. Aliferis, D. Gottesman, and J. Preskill, Quantum Inf. Comput. **6**, 97 (2006).
[83] P. Aliferis, F. Brito, D. P. DiVincenzo, J. Preskill, M. Steffen, and B. M. Terhal, New J. Phys. **11**, 013061 (2009).